Int J Appl Earth Obs Geoinformation 80 (2019) 102–114

Contents lists available at ScienceDirect

Int J Appl Earth Obs Geoinformation

journal homepage: www.elsevier.com/locate/jag

Assessing spectral measures of post-harvest forest recovery with field plot data

Joanne C. White[a,b,*], Ninni Saarinen[b,e], Michael A. Wulder[a], Ville Kankare[b], Txomin Hermosilla[a], Nicholas C. Coops[c], Markus Holopainen[b], Juha Hyyppä[d], Mikko Vastaranta[e]

[a] Canadian Forest Service, (Pacific Forestry Centre), Natural Resources Canada, 506 West Burnside Road, Victoria, BC, V8Z 1M5, Canada
[b] Department of Forest Sciences, P.O. Box 27, 00014 University of Helsinki, Finland
[c] Faculty of Forestry, University of British Columbia, 2424 Main Mall, Vancouver, BC, V6T 1Z4, Canada
[d] Department of Remote Sensing and Photogrammetry, Finnish Geospatial Research Institute FGI, National Land Survey of Finland, Geodeetinrinne 2, 02431 Masala, Finland
[e] School of Forest Sciences, University of Eastern Finland, P.O. Box-111, 80101 Joensuu, Finland

ARTICLE INFO

Keywords:
Landsat
Forest
Time series
Composite-to-Change
Seedling plot
Boreal
Regeneration

ABSTRACT

Information regarding the nature and rate of forest recovery is required to inform forest management, monitoring, and reporting activities. Delayed establishment or return of forests has implications to harvest rotations and carbon uptake, among others, creating a need for spatially-explicit, large-area, characterizations of forest recovery. Landsat time series (LTS) has been demonstrated as a means to quantitatively relate forest recovery, noting that there are gaps in our understanding of the linkage between spectral measures of forest recovery and manifestations of forest structure and composition. Field plots provide a means to better understand the linkage between forest characteristics and spectral recovery indices. As such, from a large set of existing field plots, we considered the conditions present for the year in which the co-located pixel was considered spectrally recovered using the Years to Recovery (Y2R) metric. Y2R is a long-term metric of spectral recovery that indicates the number of years required for a pixel to return to 80% of its pre-disturbance Normalized Burn Ratio value. Absolute and relative metrics of recovery at 5 years post-disturbance were also considered. We used these three spectral recovery metrics to predict the stand development class assigned by the field crew for 284 seedling plots with an overall accuracy of 73.59%, with advanced seedling stands more accurately discriminated (omission error, OE = 15.74%) than young seedling stands (OE = 49.84%). We then used field-measured attributes (e.g. height, stem density, dominant species) from the seedling plots to classify the plots into three spectral recovery groups, which were defined using the Y2R metric: spectral recovery in (1) 1–5 years, (2) 6–10 years, or (3) 11–15 years. Overall accuracy for spectral recovery groups was 61.06%. Recovery groups 1 and 3 were discriminated with greater accuracy (producer's and user's accuracies > 66%) than recovery group 2 (< 50%). The top field-measured predictors of spectral recovery were mean height, dominant species, and percentage of stems in the plot that were deciduous. Variability in stand establishment and condition make it challenging to accurately discriminate among recovery rates within 10 years post-harvest. Our results indicate that the long-term metric Y2R relates to forest structure and composition attributes measured in the field and that spectral development post-disturbance corresponds with expectations of structural development, particularly height, for different species, site types, and deciduous abundance. These results confirm the utility of spectral recovery measures derived from LTS data to augment landscape-level assessments of post-disturbance recovery.

1. Introduction

Global commitments to increase forest area are considered a key action in offsetting the impacts of climate change (Meli et al., 2017), resulting in an increased interest in monitoring the efficacy and rate of post-disturbance forest recovery. Examples of global commitments to forest restoration include the Bonn Challenge, launched in 2011 by the German government and the IUCN, and subsequently extended by the New York Declaration on Forests made at the United Nations Climate Summit of 2014. The Bonn Challenge aims to restore 150 Mha of

* Corresponding author at: Canadian Forest Service, (Pacific Forestry Centre), Natural Resources Canada, 506 West Burnside Road, Victoria, BC, V8Z 1M5, Canada.
E-mail address: joanne.white@canada.ca (J.C. White).

https://doi.org/10.1016/j.jag.2019.04.010
Received 27 February 2019; Received in revised form 11 April 2019; Accepted 12 April 2019

degraded ecosystems by 2020, and 350 Mha by 2030, with forests as the primary target for restoration (Besseau et al., 2018). On March 1, 2019, the United Nations General Assembly declared 2021–2030 as the UN Decade on Ecosystem Restoration, seeking to accelerate the implementation of existing restoration commitments (United Nations Environment Programme, 2019). Commitments such as these require significant financial investments in order to be realized (Verdone and Seidl, 2017) and the question arises as to where to intervene and pursue active restoration versus allowing natural regeneration processes to prevail. Holl and Aide (2011) posit that forest restoration targets and associated investments should be guided by baseline information on the potential for natural regeneration success at a given location, which they refer to as the "intrinsic rate of recovery". However, spatially-explicit baseline data to guide restoration investment decision making is often not readily available.

Success in forest regeneration depends upon definitions and information needs. Definitions of forest recovery—and by association, forest restoration success—are not universal (Frolking et al., 2009; Chazdon et al., 2016). Forest recovery is a process and not a state; with the structure, composition, and function of forests manifesting gradually through successional processes that occur following disturbance (Oliver and Larson, 1996; Spake et al., 2015). The point in time at which forest recovery is achieved relates to its definition and often depends on whether the information need is related to reclamation (Audet et al., 2014), silviculture (FAO, 2012), carbon (Urbano and Keeton, 2017), or ecosystem goods and services (Thompson et al., 2013), among others. Indicators of forest recovery can therefore be compositional, functional, structural, or combinations thereof (Gatica-Saavedra et al., 2017; Chazdon et al., 2016). Measurable characteristics (e.g. tree height, canopy cover) enable objective assessments of recovery and can be measured or modeled with reasonable accuracies over large areas with technologies such as airborne laser scanning (White et al., 2018).

Currently, baseline data required to assess forest recovery often rely upon field visits (e.g., visual assessments or plot installation), which can provide highly detailed and accurate information on regenerating forests, yet which are also spatially and temporally constrained (Bartels et al., 2016). It is therefore difficult to provide baseline assessments of forest recovery over large areas based on field plot data alone. For instance, in the managed forests of Finland, variability in regeneration success has primarily been assessed through controlled experiments, routine forest inventory measures, and operational regeneration surveys (Kankaanhuhta, 2014), which involve site visits to determine if stands have achieved required minimum height and density targets (Nilsson et al., 2010).

Time series of remotely sensed data can provide a useful data source for characterizing forest recovery over large areas (Frolking et al., 2009). For example, Landsat times series (LTS) data have enabled disturbance and subsequent recovery to be characterized over regions (Schroeder et al., 2007; Kennedy et al., 2012; Griffiths et al., 2014), entire nations (White et al., 2017), and the globe (Hansen et al., 2013). Free and open access to Landsat data (Woodcock et al. 2008), combined with a spatial resolution (30 m) that allows human impacts on the landscape to be accurately captured, and a rigorous cross-sensor calibration program (Mishra et al., 2016), have greatly expanded the use of LTS data for forest monitoring (Wulder et al., 2019), and for characterizing post-disturbance forest recovery (DeVries et al., 2015; Frazier et al., 2015, Pickell et al., 2016, Chu et al., 2016; Frazier et al., 2018). Questions remain however concerning the relationship between spectral indicators of forest recovery and the actual manifestation of forest structure. Due to the information content of the Landsat spectral channels used (e.g. near-infrared (NIR) versus shortwave infrared (SWIR)), different spectral indices relate different information on the recovery process (Pickell et al., 2016) and point to the need to use both short- and long-term spectral metrics of recovery in order to better understand and characterize the recovery process (Chu et al., 2016; White et al., 2017).

Airborne laser scanning (ALS) data have been used to corroborate spectral measures of recovery (White et al., 2018), providing new insights on the utility of these spectral indicators for large area assessments. White et al. (2018) defined recovery as the return of forest structure, as quantified by measurable characteristics against which target thresholds (i.e. canopy height > 5 m and cover > 10%), were applied to indicate when recovery had occurred (FAO, 2012). In their study, the Years to Recovery (Y2R) metric was used, which is derived from a fitted time series of Normalized Burn Ratio (NBR) values, post-disturbance. The Y2R metric represents the number of years required for a pixel to return to 80% of its pre-disturbance NBR value. White et al. (2018) found that 88.9% of the pixels that were considered spectrally recovered had achieved the aforementioned benchmarks of height and cover, and that errors of omission and commission were minimized.

As noted above, field visits are the main data source for forest regeneration surveys. In Finland, the establishment of new stands is an essential element of forest management, and seedling stands are monitored to determine the optimum timing of stand tending actions ultimately targeted at increasing yields. Widely distributed and systematically surveyed seedling plots provide an opportunity to inform upon spectral recovery metrics, wherein seedling plot characteristics for co-located pixels can be assessed. In this research, we examine stand conditions in seedling plots that were measured in the year the stand was considered spectrally recovered. These plots represent a 15-year period of post-harvest conditions in the boreal forests of southern Finland and allowed us to further explore the utility of spectral measures of recovery and determine those factors (e.g. dominant species, site type, height, stem density) that influence spectral recovery rates. Our objective was to improve our understanding of spectral indicators of forest recovery and their relationship to actual manifestations of forest structure and composition, as measured in the seedling plots. Specifically, we evaluated (i) if spectral measures of recovery could be used to accurately predict the stand development class of seedling plots assigned by the field crew; (ii) conversely, if seedling plot attributes could be used to predict spectral recovery rates derived from the LTS recovery metrics; and finally determine (iii) what seedling plot characteristics distinguish stands that have rapid (< 5 years) versus slow (> 10 years) rates of spectral recovery.

2. Materials and methods

2.1. Study area

At approximately 5.3 Mha, our study area in southern Finland is a complex mosaic of agricultural, forestry, and urban land use (Fig. 1; Löfman and Kouki, 2001). An estimated 65% of the study area is forested and is predominantly located within the southern boreal vegetation zone. Characterized by intensive forest management, productive forests in the study area account for 97.5% of the forest area, having a minimum growth increment of 1 $m^3\,ha^{-1}\,yr^{-1}$. Mesic heath as the dominant site type, representing 49.8% of the forest area (Natural Resources Institute of Finland, 2015). The average stem volume is 146.4 $m^3\,ha^{-1}$, with Scots pine (*Pinus sylvestris* L.; 40.2% of stem volume), and Norway spruce (*Picea abies* L. (Karst.); 38.5% of the stem volume) as main tree species. In 2016, the total cost of silvicultural activities in Finland was estimated at EUR 251 million, with approximately 109,000 ha of artificial regeneration and 27,000 ha of natural regeneration (Natural Resources Institute Finland, 2017). Approximately 60% of forests in Finland are privately owned, compared to 26% owned by the state, 9% owned by forest companies, and 5% by others (Finnish Forest Association, 2014).

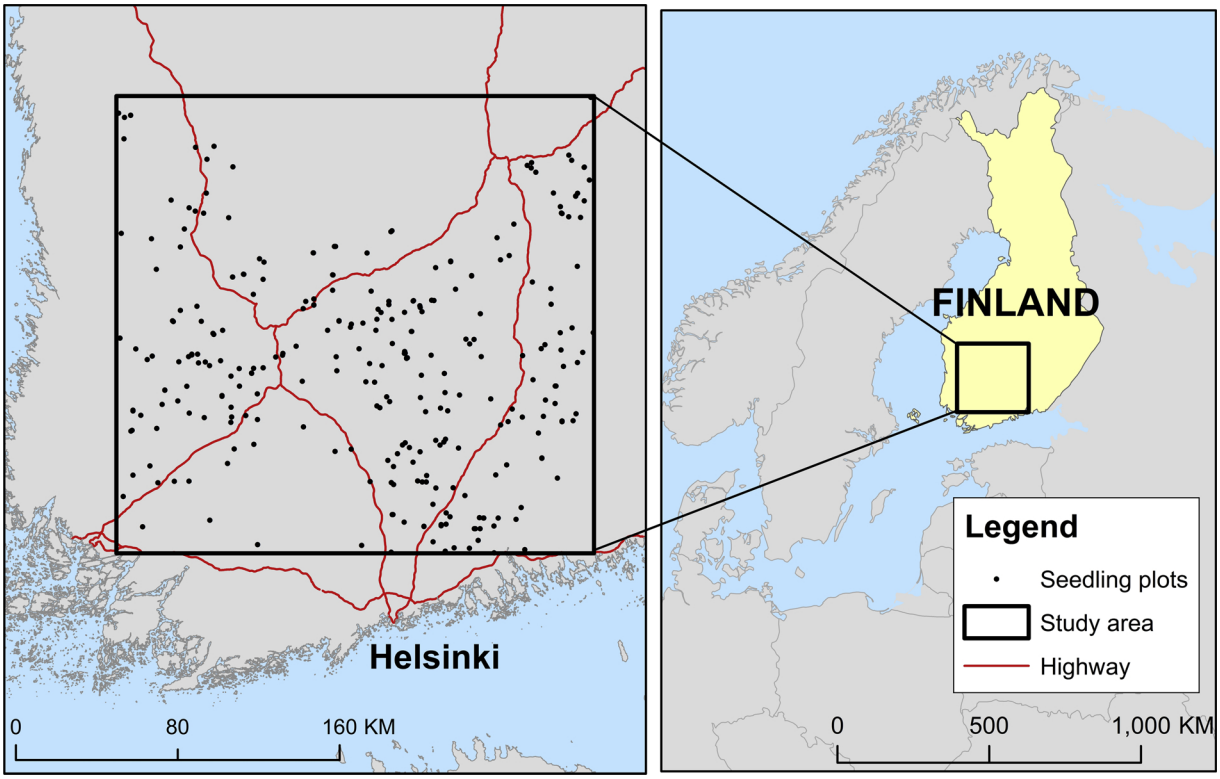

Fig. 1. Location of study area in southern Finland and spatial distribution of seedling plots used in the analysis described herein.

2.2. Data

2.2.1. Landsat time series (LTS) data

Herein we applied forest disturbance and recovery information products generated for the study area using the Composite-to-Change (C2C) approach (Hermosilla et al., 2016, 2017). Annual best-available pixel composites were generated for 1984–2017 from archived Landsat data (Saarinen et al., 2018). L1T format Landsat images were downloaded from the USGS archive and converted to surface reflectance using the LEDAPS algorithm (Masek et al., 2006; Schmidt et al., 2013), followed by clouds and cloud shadow detection and masking using the Function of mask (Fmask) algorithm (Zhu and Woodcock, 2012). After this pre-processing, each pixel in each image was assigned a score according to the compositing rules defined in White et al. (2014) and Hermosilla et al. (2016). Scores were assigned for sensor (i.e., TM, ETM + SLC-on, ETM + SLC-off, OLI), image acquisition day of year, the distance to cloud or cloud shadow, and atmospheric opacity. Scores were summed and the best pixel was selected as the pixel with the highest score; the surface reflectance value for this best observation was then written out to the annual best-available-pixel (BAP) composite. The resulting time series of annual BAP composites were then subjected to additional processing using C2C to further remove anomalous pixel values by applying a de-spiking approach (similar to Kennedy et al., 2012 and Bolton et al., 2015) and filling data gaps (i.e., pixels with no valid observations), while simultaneously identifying spectral trends and detected changes (Hermosilla et al., 2015). Spectral trends were characterized using the NBR (Key and Benson, 1999), which is calculated using the NIR and SWIR Landsat bands. NBR is considered among the most useful indices for characterizing forest change (Cohen et al., 2018). Trends were identified through piecewise linear interpolation between the temporal breakpoints detected (i.e. abrupt changes in NBR magnitude), resulting in the reduction of the residual noise in temporal trajectories (Pflugmacher et al., 2012) and the detection of changes. The subsequent output was an annual time series of gap-free surface reflectance data representing temporally fitted spectral values, and a suite of change metrics that characterize the nature of the detected changes (e.g. change magnitude, change persistence; Hermosilla et al., 2015, 2016).

Change events associated with forest harvesting were identified using change metrics and size characteristics as described in White et al. (2018). The overall accuracy of the change detection at this study site, which was characterized using visual interpretation of LTS and high resolution imagery, was 89% ± 3%, with 86% of change events detected within ± 1 year of the true change year (White et al., 2018).

2.2.2. Spectral recovery metrics

Post-disturbance recovery was assessed using spectral metrics derived from the fitted NBR time series data as per White et al. (2017, 2018; Fig. 2). The Y2R metric characterizes long-term forest regeneration and is defined as the number of years required for a pixel to return to 80% of its pre-disturbance value (Pickell et al., 2016; White et al., 2017, 2018). The pre-disturbance value is determined as the average NBR value of the 2 years prior to disturbance (y-2 and y-1):

$$NBR_{pre-disturbance} = \frac{NBR_{y-2} + NBR_{y-1}}{2} \quad (1)$$

Forest harvesting will cause a marked increase in reflectance in both the visible and SWIR bands. White et al. (2018) explored different thresholds for the Y2R metric (i.e. 60%, 80%, 100%), as well as a probabilistic approach to determine the year in which recovery was achieved, concluding that the 80% threshold provided the most realistic assessment of recovery in the boreal forests of southern Finland according to benchmarks of canopy cover and height measured with the ALS data.

In addition to the Y2R, we considered two short-term measures of recovery (Fig. 2). $\Delta NBR_{regrowth}$, which is an absolute measure of recovery at 5-years post disturbance (White et al., 2017; Fig. 2):

$$\Delta NBR_{regrowth} = NBR_{fitted,\ y5} - NBR_{fitted,\ y} \quad (2)$$

where $NBR_{fitted,y5}$ is the fitted NBR value 5-years post-disturbance and

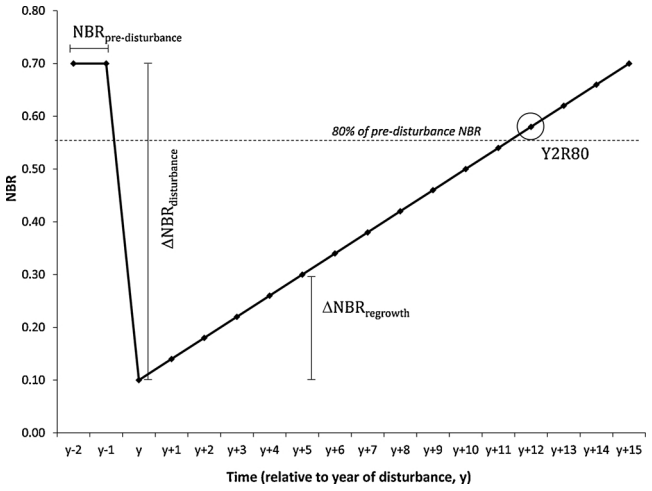

Fig. 2. A schematic of a spectral Normalized Burn Ratio (NBR) pixel series illustrating the short-term absolute ($\Delta NBR_{regrowth}$, defined in Eq. (2)) and relative (Recovery Indicator, RI, defined in Eq. (3)) spectral recovery metrics and the long-term spectral recovery metric, Y2R.

$NBR_{fitted,y}$ is the fitted NBR value in the year of disturbance.

The Recovery Indicator or RI is a relative indicate of recovery 5-years post-disturbance and is $\Delta NBR_{regrowth}$ conditioned by the magnitude of the disturbance (Kennedy et al., 2012):

$$RI = \frac{\Delta NBR_{regrowth}}{\Delta NBR_{disturbance}} \quad (3)$$

where $\Delta NBR_{regrowth}$ is defined in Eq. (2) above, and $\Delta NBR_{disturbance}$ is the C2C change magnitude (White et al., 2017; Fig. 2).

2.2.3. Seedling plot data

Data for 1310 seedling plots were obtained from the Finnish Forest Centre. Seedling stands are those with a mean height < 7 m for coniferous-dominated stands, or < 9 m for deciduous-dominated stands (Äijälä et al., 2014). Seedling stands are further divided into young (< 1.3 m) and advanced (1.3–7 or 9 m) seedling stands. Advanced seedling stands may also be discriminated based on a basal-area weighted mean diameter at breast height that is less than 8 cm, and more rarely, a maximum age that is 50 years in southern Finland (Äijälä et al., 2014). Plots had a radius of 9 m, and the location of plot centroids were measured with < 1 m accuracy. Seedling plots were selected for analysis based on two criteria: (i) the plots were located within change events identified from our C2C time series and were more than 20 m from the nearest stand boundary; and (ii) the plots were measured in the same year in which spectral recovery was indicated by the Y2R metric. The application of these criteria yielded a total of 284 plots measured from 271 different seedling stands in the summers of 2010–2017. Time since disturbance for the seedling plots ranged from 1 to 15 years. Based on the management actions recorded in the plot data, and the reported percent deciduous and stem density, there is no evidence that any thinning treatments had been applied to any of the plots. Measured plot attributes included species-level mean height and number of stems per ha for up to seven unique species-strata in each plot. Using the stratum-wise data we calculated the mean, median, maximum, and coefficient of variation (CV) of plot height, as well as the weighted mean height, whereby the number of stems in each stratum were used as weights. We also calculated the mean, median, total, and CV of stems per ha, percentage of total stems in the plot that were deciduous species (hereafter referred to as percent deciduous), and the ratio of the mean deciduous height to mean coniferous height in each plot (hereafter referred to as height ratio). Information on dominant tree species, site type, and drainage class were also recorded as categorical variables for each plot (Table 1).

Seedling plots had an average mean height of 1.98 m and an average

Table 1
Summary of measured seedling plot attributes.

Plot attribute	Summary and class codes					
	Mean	Min	Max	Lower Quartile	Upper Quartile	Std. Dev.
Mean height (m)	1.98	0.20	6.10	1.16	2.59	1.14
Weighted mean height (m)	0.86	0.05	4.00	0.41	1.08	0.70
Median height (m)	1.94	0.20	6.10	1.15	2.50	1.13
Maximum height (m)	2.52	0.20	8.40	1.50	3.50	1.45
Coefficient of variation of height (%)	28.88	0.00	118.11	14.43	40.11	19.87
Mean stems per ha	3151	367	25000	1417	3750	2842
Median stems per ha	2667	100	25000	1100	3150	2824
Maximum stems per ha	5705	500	38000	2350	7300	5190
Total stems per ha	8227	1100	38200	3850	11250	6041
Coefficient of variation of stems per ha (%)	78.51	0.00	181.67	50.91	108.73	41.31
Percent deciduous	60.35	0.00	100.00	35.00	85.25	30.37
D height: C height (Height ratio)	1.29	0.00	6.67	0.81	1.67	0.85
Dominant species	1. Scots pine (*Pinus sylvesteris* L.; n = 83) 2. Norway spruce (*Picea abies* L. Kars; n = 149) 3. Deciduous (primarily birches, *Betula* spp. L; n = 52)					
Site type	1. Heath with rich grass-herb vegetation and corresponding natural and ditched peatland (n = 66) 2. Mesic heath forest, and corresponding natural and drained peatland (n = 159) 3. Sub-xeric heath forest, and corresponding natural and drained peatland (n = 44) 4. Xeric heath forest, and corresponding natural and drained peatland (n = 15)					
Drainage class	1.Undrained mineral soil (default) (n = 244) 2. Swampy mineral soil (n = 7) 3. Drained mineral soil (n = 21) 4. Forested drained peatland (n = 12)					
Stand development class	T1. Young seedling stand, dominant height of the dominant species is < 1.3 m (n = 89); T2. Advanced seedling stand, dominant height of the dominant species is > 1.3 m (n = 195)					

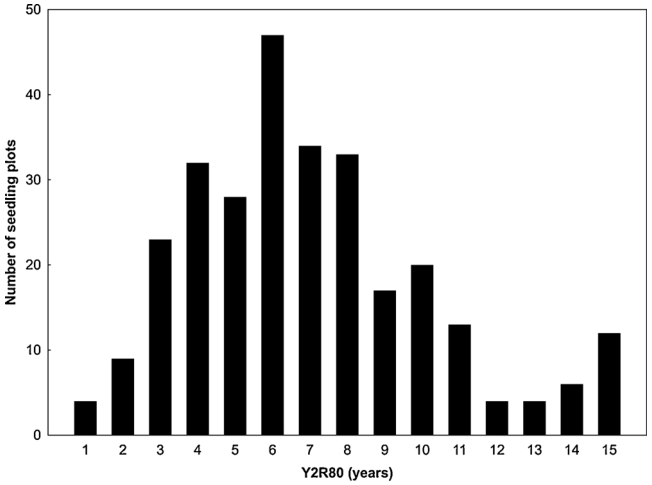

Fig. 3. Distribution of seedling plots, by Years to Recovery (Y2R) metric. This metric characterizes the number of years it takes for a plot to return to 80% of its pre-disturbance value, assessed using the Normalized Burn Ratio. Recovery groups were defined using the Y2R: (1) 1–5 years; (2) 6–10 years; (3) 11–15 years.

of 8227 total stems per ha (Table 1). Plots were composed of 60% deciduous species on average, while the average ratio of deciduous to coniferous mean heights was 1.29. The majority of seedling plots were dominated by Norway spruce (52%), and were located in mesic heath forest site types (56%). The regeneration stage in northern Europe is characterized as that period of time between final felling and when the main tree species established at a site has attained an average height of 1.3 m (Nilsson et al., 2010), which in Finland is considered the young seedling stand development class (Table 1; Äijälä et al., 2014). Approximately 69% of the seedling plots used in our analysis were classified as young seedling stands, and the remaining 31% were classified as advanced seedling stands. Additionally, the target stem density for regenerated stands is a minimum of 1800–2500 stems per ha, although this target is frequently not met (Nilsson et al., 2010). 90% of the seedling plots used in our analysis had total stems per ha > 2500. The Finnish Forest Act obligates forest owners to regenerate forests after the final felling is complete and defines the minimum density and height that must be attained within 10 years from the final felling (Ministry of Agriculture and Forestry, 1996, 2010). The mean height must be greater than 0.5 m, and the minimum number of stems per ha is 1300 for Scots pine, 1200 for Norway spruce, and 1000 for deciduous. Approximately 98% of our pine-dominated plots and 100% of our spruce and deciduous plots met these criteria. From this we conclude that our seedling plots were representative of successfully regenerated stand conditions following final harvest.

Previous research characterizing forest recovery post-disturbance (e.g., Bartels et al., 2016 for plot-based recovery studies in boreal forests of Canada) has indicated that time to recovery is highly variable and is influenced by many factors including site characteristics and disturbance magnitude. As a result of this variability, regulatory frameworks often specify broad time frames within which regeneration targets may be achieved (e.g. within 10 years post-harvest in Finland). For this reason, White et al. (2018) based their assessment of spectral recovery with ALS data on temporal recovery groups rather than individual Y2R (i.e. < 10 years, 10–13 years, 14–17 years, > 17 years). In this study, we uniquely had a 15 year recovery period available for analysis, for which we had field plots measured in the year the plot was considered spectrally recovered by the Y2R metric. Accounting for the known variability in recovery rates, while also wanting to investigate variation within the initial 10-year window post-harvest, we opted to divide our seedling plots into three equal 5-year spectral recovery groups based on their Y2R value (Fig. 3): (1) 1–5 years (n = 94), (2) 6–10 years (n = 151), and (3) 11–15 years (n = 39). We evaluated the mean values of $NBR_{pre\text{-}disturbance}$ for our three spectral recovery groups and found no statistically significant difference in pre-disturbance NBR spectral conditions among the three recovery groups($F_{(2,281)} = 2.01$, $p = 0.13$).

2.3. Analysis methods

2.3.1. Predictive models

To evaluate the utility of using LTS recovery metrics $\Delta NBR_{regrowth}$, RI, and Y2R for predicting the stand development class of the seedling plots, we generated a random forest model (Breiman, 2001) with seedling plot development classes as response variables and the three LTS recovery metrics (i.e., $NBR_{regrowth}$, RI, Y2R) as predictors. Conversely, to determine if seedling plot attributes could be used to discriminate spectral recovery rates, we generated a random forest model that classified the seedling plots into three spectral recovery groups defined using the Y2R metric (i.e., 1–5 years, 6–10 years, 11–15 years; Fig. 3). Random forests is a robust classifier that often outperforms other classification algorithms (Fernandez-Delgado et al., 2014), and that is readily parameterized, robust to overfitting, and can directly incorporate both categorical and continuous predictors (Belgiu and Drăgut, 2016). Predictor selection for the spectral recovery group model is described below. For both models, random forests was implemented using the R package *caret* (Kuhn, 2018; Liaw and Weiner, 2002, 2018), with the number of trees to grow (*ntree*) set to 1000, and the number of variables to use at each split (*mtry*) optimized within *caret*. Finally, to determine those field-measured characteristics associated with plots that have slow and fast rates of spectral recovery we analyzed the variance in continuous seedling plot attributes by recovery group, and for the categorical seedling plot attributes (i.e., species, site type, and drainage) variance in Y2R was analyzed.

2.3.2. Predictor selection

Correlation between predictors has been demonstrated to influence variable importance measures in random forests, particularly when variables have different scales of measurement or numbers of categories (Strobl et al., 2007, 2008). Moreover, correlation between predictors can dilute the importance of key predictors (Kuhn and Johnson, 2013). The seedling plot attributes represent a mix of continuous and categorical measures (Table 1). Predictors for the spectral recovery groups model were selected by assessing the degree of correlation among the continuous seedling plot attributes (using Pearson's *r*), as well as between the continuous seedling plot attributes and Y2R. The conditional measure of variable importance from *cforest* (Strobl et al., 2009), was also used to evaluate predictors. Independent sample t-tests were used to test for significant differences between young and advanced seedling stand development classes for the three spectral recovery metrics. Likewise, one-way ANOVA and post-hoc Tukey tests were used to test for significant differences in continuous seedling plot attributes among the three recovery groups, and to test for significant differences in Y2R for categorical seedling plot attributes.

2.3.3. Model validation

For validation of the classification outcomes, we followed the recommendation of Kuhn and Johnson (2013) and applied a 10-fold cross-validation, repeated 5 times in *caret*, resulting in 50 different hold-out datasets or folds for assessing model performance. Confusion matrices were generated to report overall accuracy, as well as omission and commission errors for each of the recovery groups. Class allocations in the confusion matrices represented the average across all folds (Kuhn, 2018).

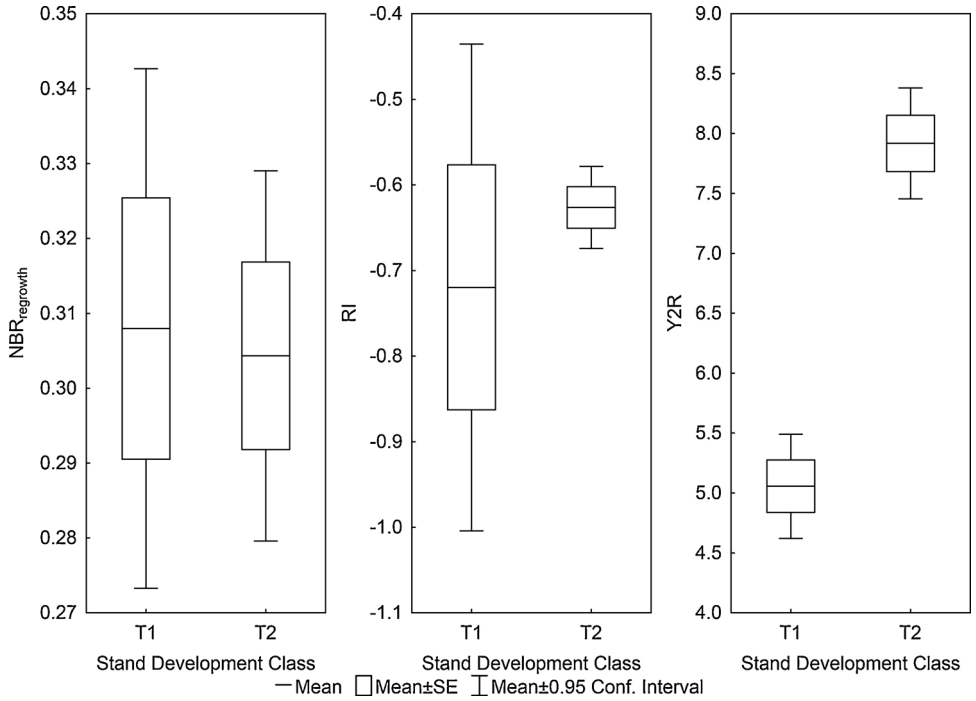

Fig. 4. Landsat times series metrics of the absolute ($\Delta NBR_{regrowth}$) and relative (RI) measure of spectral recovery at 5 years post-disturbance as well as Years to Recovery (Y2R), by stand development class of young (T1) and advanced (T2) seedling stands.

Table 2
Confusion matrix for classification of stand development class. T1 = young seedling stand; T2 = advanced seedling stand.

	Observed				
Predicted	T1	T2	Total	User's accuracy	Commission error
T1	45	31	75	59.25%	40.75%
T2	44	164	208	78.75%	21.25%
Total	89	195	209		
Producer's accuracy	50.16%	84.26%		Overall accuracy	Margin of error:
Omission error	49.84%	15.74%		73.59%	± 5.11%

3. Results

3.1. Prediction of stand development class

Correlation among the three LTS recovery metrics was low ($r < 0.3$). Independent sample t-tests indicated that there was no statistically significant difference between young seedling stands and advanced seedling stands for $NBR_{regrowth}$ ($t_{(282)} = 0.16$, $p = 0.86$) or RI ($t_{(282)} = 0.91$, $p = 0.36$), but there was a statistically significant difference for Y2R ($t_{(282)} = 7.56$, $p = 0.00$) (Fig. 4). The LTS metrics discriminated the two stand development classes with an overall accuracy of 73.59% ± 5.11% (Table 2). Advanced seedling stands were distinguished with markedly greater accuracy than young seedling stands, with a producer's accuracy of 84.26% for advanced seedling stands, compared to only 50.16% for young seedling stands. Omission and commission errors were 52% and 41% for young seedling stands respectively, compared to 16% and 21% for advanced seedling stands (Table 2). Y2R was the most important predictor of stand development class, followed by RI and $NBR_{regrowth}$, with variable importance scores of 63.2%, 39.13%, and 17.57%, respectively. The average trajectories for each spectral recovery group and associated spectral recovery metrics are shown in Fig. 5.

3.2. Prediction of spectral recovery groups

Correlation amongst potential predictors from the seedling plot attributes were greatest among the various height and stem density attributes (Table 3). Conditional variable importance measures from a preliminary model run of *cforest* indicated that mean height was the most important height attribute for predicting spectral recovery groups and the CV of stem density was the most important density attribute; these attributes also had the highest correlation with Y2R (Table 3). There were no strong correlations ($r \geq 0.6$) between height and stem density attributes or among the other plot attributes. The final set of selected predictors included mean height, CV in stem density, height ratio, percent deciduous, dominant species, site type, and drainage class. The variable importance measures for each of the predictors were as follows: mean height (100%), dominant species (17.51%), percent deciduous (6.49%), height ratio (5.60%), site type (4.37%), coefficient of variation of stem density (1.96%), and drainage (0%).

Using the selected seedling plot attributes, the three spectral recovery groups were discriminated with an overall accuracy of 61.06% (± 5.67%; Table 4). Producer's accuracy was 70.51% and 68.69% for recovery groups 1 and 3, respectively, but was 43.64% for recovery group 2. Likewise, user's accuracies were comparable for recovery groups 1 and 3 (˜66%), and lower for recovery group 2 (48.95%). Confusion was greater between recovery groups 1 and 2. Conversely, there was relatively minor confusion between recovery groups 1 and 3.

3.3. Seedling plot attributes influencing spectral recovery

One-way ANOVAs indicated significant differences in mean height among spectral recovery groups ($F_{(2,281)} = 50.96$, $p = 0.00$), and post-hoc Tukey tests indicated that there were significant differences in mean height amongst all three recovery groups (Fig. 6). The average mean height for recovery group 1 was 1.4 m, compared to 3.29 m for recovery group 3. There were also significant differences in percent deciduous ($F_{(2,281)} = 7.29$, $p = 0.00$) by recovery group, and post-hoc

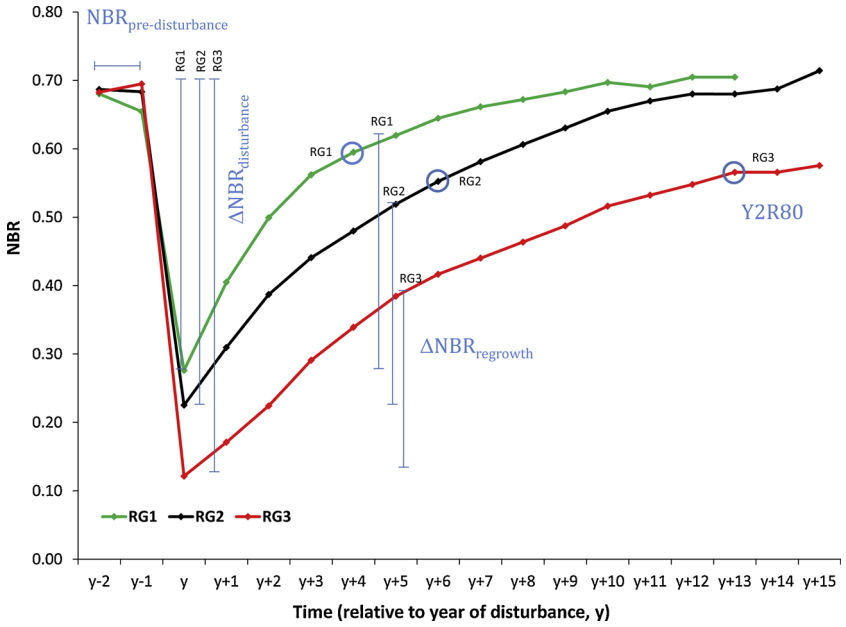

Fig. 5. Average spectral trajectories for each of the three spectral recovery groups: RG1 = spectral recovery in 1–5 years, RG2 = 6–10 years, RG3 = 11–15 years).

Table 3
Correlation among seedling plot attributes and Years to Recovery (Y2R) metric. H = height, wmean = weighted mean, cv = coefficient of variation, N = number of stems per ha, dht_cht = ratio of the mean deciduous height to mean coniferous height, per_d = percentage of total stems in the plot that were deciduous species. Predictors used in the final model indicated in bold.

	mean_H	wmean_H	median_H	max_H	cv_H	mean_N	median_N	max_N	total_N	**cv_N**	**dht_cht**	**per_d**	Y2R
mean_H	1.00												
wmean_H	0.79	1.00											
median_H	0.98	0.79	1.00										
max_H	0.93	0.64	0.87	1.00									
cv_H	0.16	0.28	0.20	0.11	1.00								
mean_N	0.16	0.01	0.14	0.22	0.17	1.00							
median_N	0.16	0.04	0.13	0.23	0.18	0.92	1.00						
max_N	0.16	0.11	0.14	0.18	0.07	0.89	0.69	1.00					
total_N	0.23	0.25	0.22	0.24	0.02	0.83	0.65	0.92	1.00				
cv_N	0.01	0.26	0.04	0.08	0.21	0.09	0.12	0.42	0.32	1.00			
dht_cht	0.16	0.28	0.18	0.04	0.59	0.08	0.12	0.04	0.11	0.29	1.00		
per_d	0.08	0.12	0.08	0.09	0.06	0.38	0.29	0.47	0.50	0.29	0.20	1.00	
Y2R	**0.59**	0.40	0.58	0.55	0.11	0.18	0.20	0.15	0.17	**0.32**	**0.08**	**0.21**	1.00

Table 4
Confusion matrix for 5-year spectral recovery groups. RG1 = spectral recovery in 1–5 years, RG2 = 6–10 years, RG3 = 11–15 years.

	Observed					
Predicted	RG1	RG2	RG3	Total	User's accuracy	Commission error
RG1	71	33	3	107	66.40%	33.60%
RG2	19	41	24	84	48.95%	51.35%
RG3	11	20	61	92	66.15%	33.85%
Total	101	94	89	173		
Producer's accuracy	70.51%	43.64%	68.69%		Overall accuracy	Margin of error:
Omission error	29.49%	56.36%	31.31%		61.06%	± 5.67%

Tukey tests indicated significant differences between recovery groups 1 and 3, and groups 2 and 3, but not between groups 1 and 2 (Fig. 6). The average percentage of stems that were deciduous in recovery group 1 was 69%, compared to 49% for group 3. No significant differences were found between recovery groups for CV in stem density ($F_{(2,281)} = 0.329$, $p = 0.72$) (Fig. 6); however, there were significant differences in total stem density ($F_{(2,281)} = 3.74$, $p = 0.02$) between groups 1 (mean = 9322 stems) and 3 (mean = 6264 stems).

Although no significant differences were found among recovery groups for height ratio ($F_{(2,281)} = 0.78$, $p = 0.46$) (Fig. 6), we found that the relationship between the deciduous and coniferous mean plot heights varied by recovery group, with a stronger relationship between coniferous and deciduous mean heights for those plots that recovered within 1–5 years (recovery group 1; r = 0.78), compared to plots that recovered in 11–15 years (recovery group 3; r = 0.54; Fig. 7).

A one-way ANOVA indicated significant differences in mean Y2R values among dominant species ($F_{(2,283)} = 12.91$, $p = 0.00$). Post-hoc Tukey tests revealed that there were significant differences ($p < 0.05$) in Y2R between Scots pine (mean = 8.4 years, sd = 3.6 years) and both Norway spruce (mean = 6.2 years, sd = 2.7 years) and deciduous species (mean = 6.7 years, sd = 3.1 years), but not between Norway Spruce and deciduous dominated plots (Fig. 8). Likewise, we found significant differences in Y2R among site types ($F_{(3,282)} = 6.77$, $p = 0.00$), with a post-hoc Tukey test indicating significant differences ($p < 0.05$) in Y2R between heath (mean = 6.1 years, sd = 2.6 years) / mesic heath (mean = 6.7 years, sd = 3.3 years) site types, and the sub xeric (mean = 8.3 years, sd = 3.2 years)/xeric (mean = 9.2 years, sd = 3.4 years) site types. Examples of stand conditions for the three

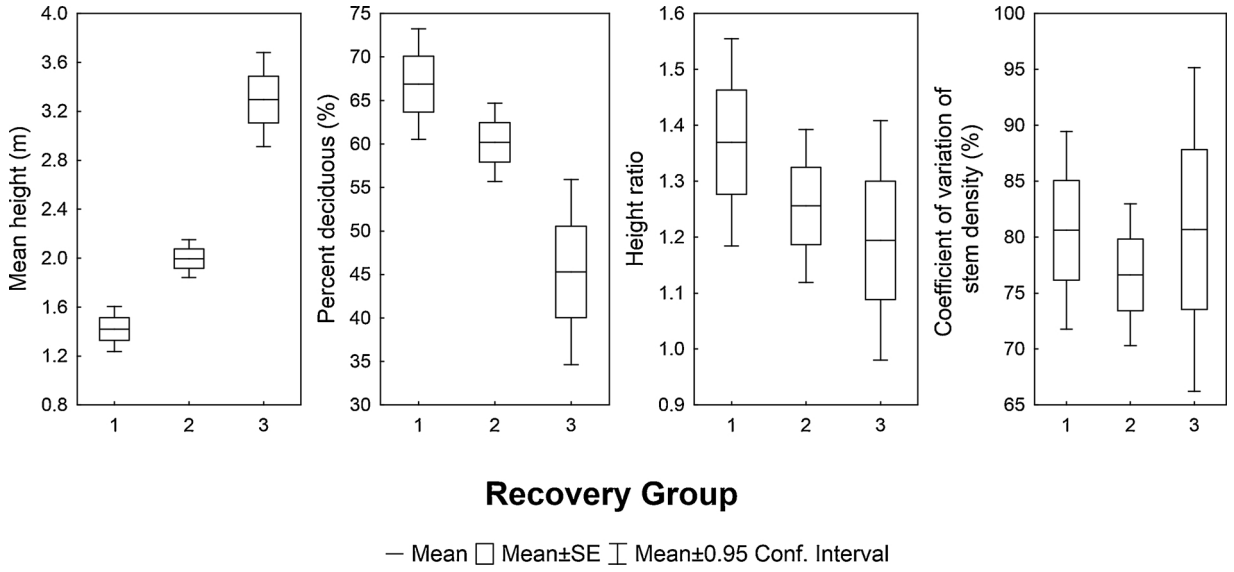

Fig. 6. Continuous seedling plot attributes used to discriminate spectral recovery groups; 1 = spectral recovery in 1–5 years, 2 = 6–10 years, 3 = 11–15 years.

recovery groups are provided for mesic heath and xeric site types in Fig. 9.

4. Discussion

In the context of increasing global interest in forest restoration, LTS data provide the opportunity to characterize forest recovery over large areas in a manner that is spatially-explicit and at a spatial resolution (30 m) that is spatially relevant for monitoring and management. However, a disconnect remains in our understanding of how spectral measures of recovery relate to actual manifestations of forest structure and composition. Herein, we addressed this knowledge gap by using seedling plots that were measured in the year the plot was considered as spectrally recovered by the Y2R metric (White et al., 2018). Forest regeneration in this boreal environment varies markedly by year, location, and site, soil condition (e.g., moisture, texture), proximity to mature forest stands, dominant climate regime, and weather during the initial growing season (Saksa et al., 2013), as well as the degree and nature of management intervention in the regeneration process (Kankaanhuhta et al., 2010). Variability in seedling plot conditions have presented challenges in estimating regeneration success (Miina and Saksa, 2013) and in predicting the need for seedling stand tending (Korhonen et al., 2013; Miina et al., 2018).

Stand development class is an attribute assigned in the field, with young seedling stands identified as those stands for which the dominant tree storey is less than 1.3 m. In our plots, young seedling plots had an average of 9382 total stems per ha and an average mean height of 1.04 m (sd = 0.6 m). Advanced seedling plots were typically less dense and taller than the young seedling plots, with an average of 7699 total stems per ha and an average mean height of 2.44 m (sd = 1.05 m). We used both short- and long-term metrics of spectral recovery to classify the seedling plots into these two development classes with an overall accuracy of 73.59%; however, our results indicated that the advanced seedling stands were discriminated more accurately than the young seedling stands. The short-term absolute ($NBR_{regrowth}$) and relative (RI) metrics of recovery at 5 years did not differ significantly between the

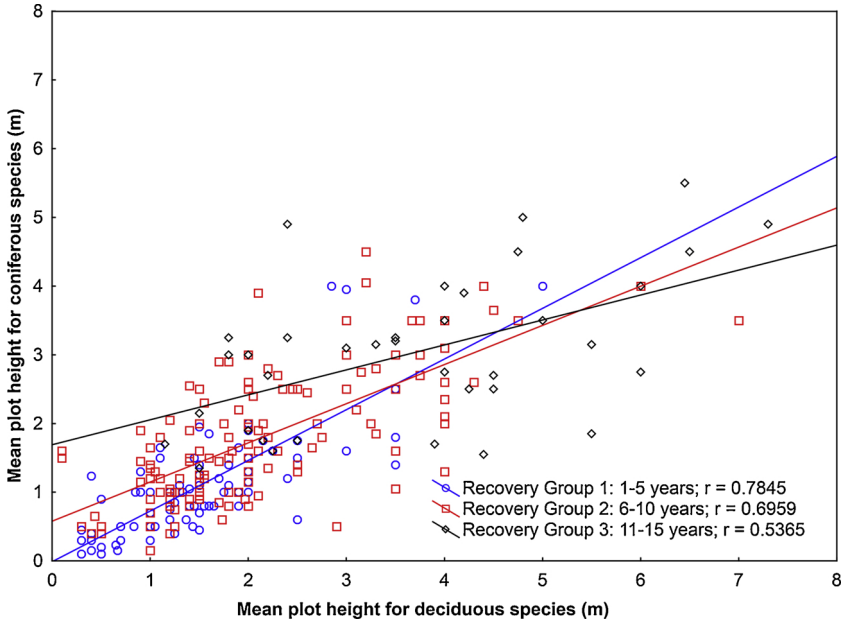

Fig. 7. Scatterplot of mean deciduous versus mean coniferous plot heights, by recovery group.

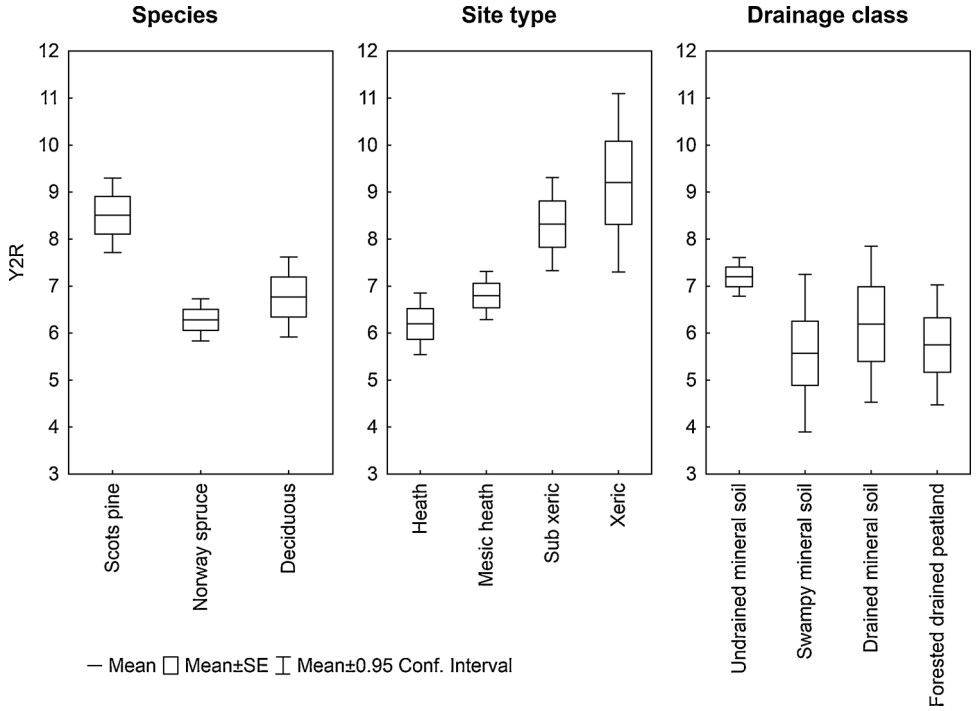

Fig. 8. Difference in average Years to Recovery (Y2R) metric by species, site type, and drainage class.

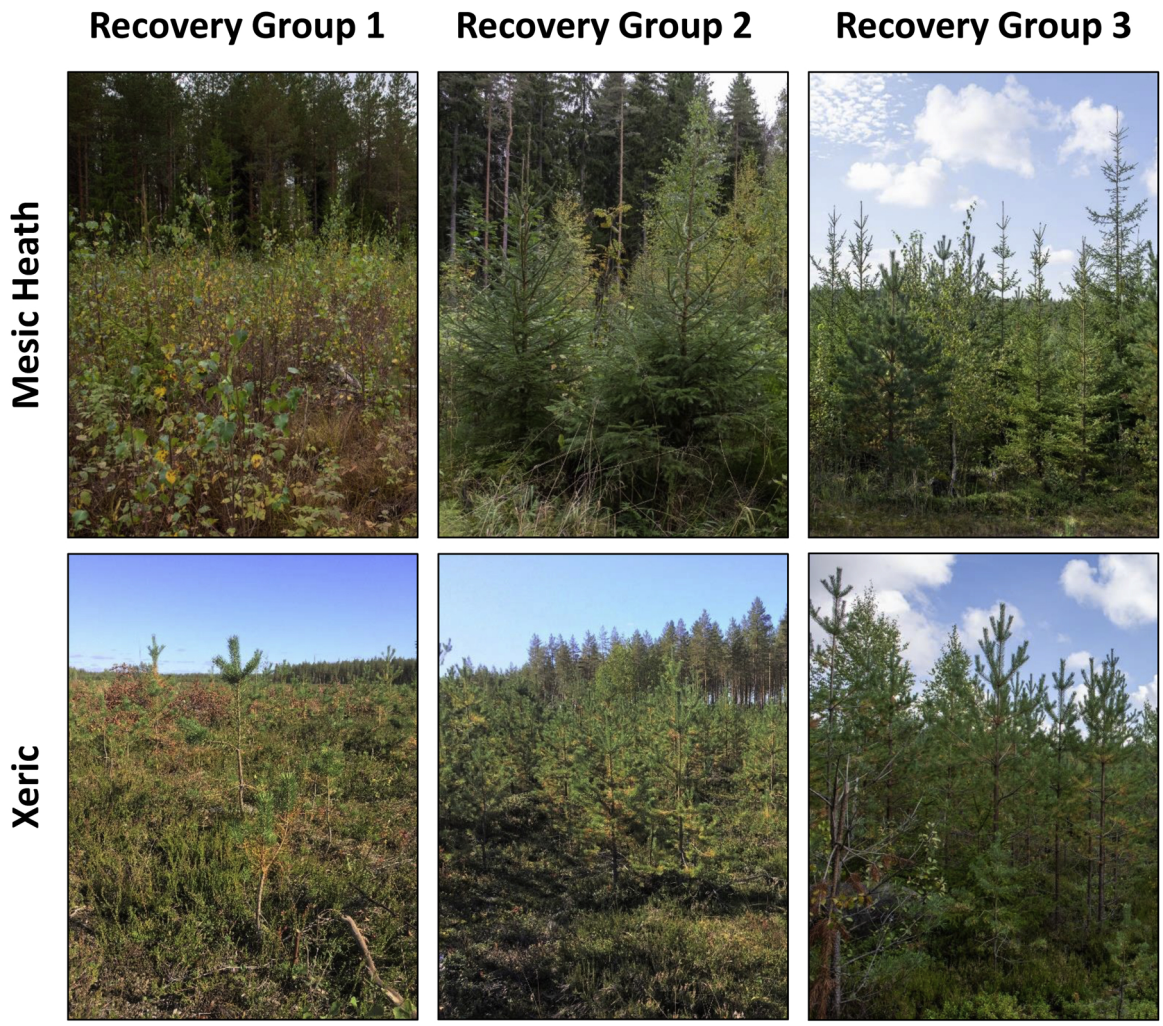

Fig. 9. Examples of the three recovery groups for the mesic heath and xeric site types.

stand development classes; however, the young seedling stands are characterized by a much broader distribution in metric values relative to advanced seedling stands, particularly for RI (Fig. 4). The relative importance of RI to discriminating between the stand development classes is worth noting, as it suggests that a spectral measure of recovery at a single point in time, early in the regeneration phase (i.e., at 5 years), may be informative of longer-term trends in recovery, an idea that was initially put forward in an LTS context by Kennedy et al. (2012). Finally, as indicated by the average spectral trajectories shown in Fig. 5, there are differences in change magnitude ($\Delta NBR_{disturbance}$) among the three recovery groups, and change magnitude can influence recovery rates (Franklin et al., 2002; Bartels et al., 2016).

We then used plot-measured attributes to discriminate the seedling plots into three spectral recovery groups, which were defined by 5-year groupings of the Y2R metric. Overall accuracy for this model was moderate at 61.06%. Mean height was the most important predictor of spectral recovery group, followed by dominant species, percentage of stems that were deciduous, ratio of deciduous to coniferous mean heights, and site type. The greatest classification confusion was in discriminating those plots that spectrally recovered in 6–10 years; plots that recovered in 1–5 years or 11–15 years were discriminated with greater accuracy.

Initially, height growth in newly established trees is slow until the tree accumulates sufficient energy for growth of its terminal shoot, after which time the tree can experience rapid height growth (Oliver and Larson, 1996). While height may be a useful indicator of recovery, height is also the structural manifestation of other site factors that influence the recovery process, and different tree species will have different patterns of height growth (Oliver and Larson, 1996). Our analysis indicated that there were significant differences in mean plot height amongst all three spectral recovery groups, but pragmatically, the difference in mean height between groups 1 and 2 was only ˜0.5 m, whereas the difference in mean plot heights between groups 1 and 3 was 2.5 m. The influence of height on spectral properties has been noted by others (Horler and Ahern, 1986; Nilson and Peterson, 1994; Olsson, 2009). Height is often used as an indicator of recovery (Bartels et al., 2016; White et al., 2018) and is fundamental to many definitions of forests (Chazdon et al., 2016). Our plots were selected to convey stand structural characteristics in the year in which the stands were considered to be spectrally recovered. Our plots in this study therefore represent a chronosequence of spectral recovery, explaining the differences in mean plot height by recovery group (Fig. 6) and align with expectation of height development in newly established stands (Oliver and Larson, 1996). White et al. (2018) examined the heights of stands that were harvested in 1991 (using ALS data in the same study site in southern Finland as used herein). Stands that had rapid spectral recovery (i.e. < 10 years) had significantly larger median values for ALS height percentiles (75th, 90th, 95th, and 99th) relative to stands that took longer to recover. Hence, stands that recovered rapidly were taller on average at the time of ALS measurement, than stands that took longer to recover. Kuusinen et al. (2016) likewise reported that ALS-measured height had the strongest linear correlation with short-wave forest albedo for plot data in central Finland.

There were also significant differences in spectral recovery between species and site types, with Norway spruce and deciduous-dominated plots having significantly shorter spectral recovery rates than Scots pine-dominated plots (Fig. 8). Likewise, the more productive heath and mesic heath site types spectrally recovered more rapidly than xeric and sub xeric site types (Fig. 8). In Finland, the main commercial tree species are Norway spruce, Scots pine, and silver birch. Scots pine is regenerated primarily on sites of medium to low fertility (i.e., sub-xeric and xeric sites), whereas Norway spruce and silver birch are regenerated primarily on more fertile sites (i.e., heath and mesic heath). Ekö et al. (2008) found that the growth difference of Scots pine compared to Norway spruce in southern Sweden was ˜60%, and for birch compared to Scots pine was ˜70%. Other studies have found that under more controlled conditions, Scots pine can have more rapid growth, but was also found to be susceptible to damage for a longer period when compared to Norway spruce (Johansson et al., 2015). Moreover, it is increasingly common for Scots pines to be regenerated from seed, whereas Norway spruces are more commonly regenerated from seedlings of 20–30 cm in height (Miina and Saksa, 2013). Eerikäinen et al. (2014) also found that Scots pine has higher mortality than either Norway spruce or birch. The influence of site quality on regeneration success in Finland has likewise been documented by others (Cajander, 1909; Ilvessalo et al., 1975; Kankaanhuhta et al., 2009). As different species are typically regenerated on different site types, it is difficult to disentangle the influence of these factors on spectral recovery. Nilson and Peterson (1994) identified species composition of the dominant canopy layer was the main driver of reflectance development over time.

We found that variability in spectral recovery was also influenced by the amount of deciduous tree species that establish at a site, as well as the heights of those deciduous species relative to the coniferous stems present at the site. In the study area, deciduous species commonly regenerate naturally and often establish prior to the planting of spruce or pine seedlings. As indicated in Fig. 6, an abundance of deciduous species in a plot influences the rates of spectral recovery. On average, seedling plots in recovery group 1 had a higher percentage of deciduous stems (66%), than recovery group 3 (45%; Fig. 6). As noted by Bartels et al. (2016), regeneration by remnant species at a site can influence recovery rates, with deciduous species that regenerate vegetatively establishing much more quickly at a site than species that regenerate from seed. In turn, these deciduous species can grow rapidly on productive sites, further influencing assessments of recovery rates that use height thresholds as an indicator of recovery. The presence of understorey will also influence spectral recovery rates, and understorey can be more abundant on fertile sites. Kuusinen et al. (2014) found that the spectral bi-directional reflectance function of sunlit understory in boreal forests of southern Finland varied according to the stand development and site fertility, as well as between Scots pine and Norway spruce. Similar variation has been documented in boreal forests of North America (Miller et al., 1997). Variation in the establishment of understorey vegetation in the initial period post-disturbance will influence spectral response in these young seedling stands (Song et al., 2007), unfortunately, no information regarding the type or abundance of understorey vegetation is recorded for the seedling plots. Likewise, no information is available on the amount of residual vegetation or trees remaining following final harvest. In Finland, forest certification requires that 10 retention trees are left for every hectare of clearcut and as approximately 85% of Finnish commercial forests are certified (Forest Stewardship Council Finland, 2010; PEFC Finland, 2014) retention trees can be expected in the stands included in this study. Typically however, seedling plots are established to exclude retention trees.

Our previous synthesis of recovery rates in the Canadian boreal forests using field plot observations indicated that harvested areas attained benchmarks of cover (10%) and height (5 m) in < 10 years, but that there was substantial variation in attainment of these benchmarks (Bartels et al., 2016). Our subsequent analyses using the Y2R metric to provide a national assessment of recovery in Canadian forests indicated an average of 6.6 years to achieve spectral recovery ($\sigma = 3.9$ years) for harvested areas, compared to 10.6 years ($\sigma = 5.6$ years) for wildfire areas. Based on this knowledge, White et al. (2018) grouped Y2R < 10 years as a single group for a subsequent assessment of recovery in southern Finland against benchmark targets of cover and height derived from ALS data. Olsson (2009) modelled the development of young boreal plantations in northern Sweden with LTS data, but due to variability in spectral response, models of spectral trends were not initiated until 5 years post-harvest. In this study, we have attempted to examine recovery within that initial 10-year window post-disturbance and distinguish between plots that recover in < 5 years versus those that recover in > 5 years. While we were able to discriminate those

stands that spectrally recovered in < 5 years from those that took > 10 years, there was substantial confusion between recovery groups 1 and 2. Our results suggest that the practice of grouping those areas that achieve spectral recovery in < 10 years in this forest environment is reasonable from a management or reporting perspective. A 10-year threshold also coincides with the regulatory timeframes concerning regeneration that are established in Finnish legislation (Ministry of Agriculture and Forestry, 1996, 2010).

The overall accuracy with which the seedling plots could be assigned to 5-year recovery groups was moderate. In addition to the variability in plot conditions within the first 10 years post-disturbance that we observed in our data, the attributes typically acquired in seedling plots may not capture other factors that also influence reflectance recovery trajectories in newly establishing stands (Nilson and Peterson, 1994). For example, information on the nature and abundance of understorey vegetation or the amount (and size) of retention trees left in the stand would likely also be informative for understanding spectral recovery rates. Nevertheless, the relationship observed herein between fast and slow recovery rates and seedling plot attributes such as height, species, and site type indicate that spectral recovery is influenced by differences in stand structural and compositional characteristics. In the context of large-area, spatially-explicit estimates of forest recovery generated from LTS data, composition should be considered if the information need is to characterize regeneration of specific forest types.

To date, the spectral metrics considered herein have primarily been tested in boreal forests, and their applicability to other forest environments remains to be determined. Estimates of forest height and cover derived from ALS data can provide useful benchmarks for assessing these spectral metrics in these environments. Future investigations should prototype the approach presented herein in areas with both slow and fast recovery in order to demonstrate (i) that spectral recovery estimates can successfully identify forest areas that have slower than expected recovery; and (ii) that this information can support spatially-explicit restoration or reforestation planning efforts. Finally, the approach presented herein relies on a temporal archive of calibrated observations and a long baseline, such as that provided by Landsat data (Belward and Skøien, 2015). Efforts to cross-calibrate and harmonize Sentinel-2 data with Landsat (Claverie et al., 2018) offer opportunities to further extend this baseline, increasing near-term temporal density and the likelihood of cloud-free imagery (Wulder et al., 2015). Thus, the integration of Sentinel-2 data into LTS post-disturbance recovery assessments also merits investigation.

5. Conclusion

LTS data provide opportunities to monitor forest recovery over large areas in a consistent and transparent manner. Such monitoring capacity for regenerating forests is useful for forest restoration efforts in the context of climate change, and for closing the disturbance loop in order to more fully characterize forest dynamics at the landscape level. Understanding the relationships between spectral recovery and the recovery of forest structure and composition is a useful precursor to the widespread application of such monitoring approaches. As a process, forest recovery is a highly variable, and monitoring efforts require definitions of recovery that are tied to the information need and the management context, as well as clear linkages between spectral recovery metrics and measurable indicators of forest structure, composition, or function. Herein, we have related field plot measurements to spectral measures of recovery and provided insights on those structural or compositional factors that influence the rate of spectral recovery within the first 15 years of stand development post-disturbance in the boreal forests of southern Finland. We found that of the field plot attributes we assessed, mean height was the most important predictor of forest spectral recovery, thereby linking structural development with spectral indicators of recovery. However, we also found that other factors, such as species and the percentage of stems in a plot that were deciduous, were also useful for discriminating amongst different recovery groups. Importantly, we observed that recovery, whether it is measured spectrally or in the field, is highly variable within the first 10-years of stand establishment. Therefore, attempting to discriminate amongst different spectral recovery rates for stands < 10 years in this forest environment may not be possible with sufficient accuracy to be informative for management. Finally, we confirm that the Y2R provides a useful assessment of spectral recovery that links to structural and compositional attributes measured in the field and expectations of stand development post-harvest and should be further explored as a monitoring indicator for forest recovery in other forest environments.

Acknowledgements

This research was undertaken as part of the “Earth Observation to Inform Canada’s Climate Change Agenda (EO3C)” project jointly funded by the Canadian Space Agency (CSA), Government Related Initiatives Program (GRIP), and the Canadian Forest Service (CFS) of Natural Resources Canada. This research was enabled in part by support provided by WestGrid (www.westgrid.ca) and Compute Canada (www.computecanada.ca) with additional support from a Natural Sciences and Engineering Research Council (NSERC) Discovery Grant to N. Coops, and from the Academy of Finland through the Centre of Excellence in Laser Scanning Research (project number 272195). G. Hobart is thanked for his assistance in acquiring the Landsat data and preparing the annual best-available pixel image composites. We appreciate the time and efforts of the Editor and two anonymous reviewers, whose constructive comments enabled improvments to this manuscript.

References

Äijälä, O., Koistinen, A., Sved, J., Vanhatalo, K., Väisänen, P. (Eds.), 2014. Metsänhoidon suositukset. Metsätalouden kehittämiskeskus Tapion julkaisuja, Available online (in Finnish only): (accessed August 16, 2018). https://www.metsanhoitosuositukset.fi/wp-content/uploads/2016/08/Metsanhoidon_suositukset_Tapio_2014.pdf.

Audet, P., Pinno, B.D., Thiffault, E., 2014. Reclamation of boreal forest after oil sands mining: Anticipating novel challenges in novel environments. Can. J. For. Res. 45, 364–371.

Bartels, S.F., Chen, H.Y.H., Wulder, M.A., White, J.C., 2016. Trends in post-disturbance recovery rates of Canada’s forests following wildfire and harvest. For. Ecol. Manage. 361, 194–207.

Belgiu, M., Drăgut, L., 2016. Random forest in remote sensing: a review of applications and future directions. ISPRS J. Photogramm. Remote. Sens. 114, 24–31.

Belward, A.S., Skøien, J.O., 2015. Who launched what, when and why: trends in global land-cover observation capacity from civilian earth observation satellites. ISPRS J. Photogramm. Remote. Sens. 103, 115–128.

Besseau, P., Graham, S., Christophersen, T. (Eds.), 2018. Restoring Forests and Landscapes: the Key to a Sustainable Future. Global Partnership on Forest and Landscape Restoration, Vienna, Austria. Available online: http://www.forestlandscaperestoration.org/sites/forestlandscaperestoration.org/files/resources/GPFLR_FINAL%2027Aug.pdf [accessed April 9, 2019].

Bolton, D.K., Coops, N.C., Wulder, M.A., 2015. Characterizing residual structure and forest recovery following high-severity fire in the western boreal of Canada using Landsat time-series and airborne LiDAR data. Remote Sensing of Environment 163, 48–60.

Breiman, L., 2001. Random forests. Mach. Learn. 45, 5–32.

Cajander, A.K., 1909. Über Waldtypen. Acta For. Fenn. 1, 1–175.

Chazdon, R.L., Brancalion, P.H.S., Laestadius, L., Bennett-Curry, A., Buckingham, K., Kumar, C., Moll-Rocek, J., Guimarães Vieira, I.C., Wilson, S.J., 2016. When is a forest a forest? Forest concepts and definitions in the error of forest and landscape restoration. Ambio 45, 538–550.

Chu, T., Guo, X., Takeda, K., 2016. Remote sensing approach to detect post-fire vegetation regrowth in Siberian boreal larch forest. Ecol. Indic. 62, 32–46.

Claverie, M., Ju, J., Masek, J.G., Dungan, J.L., Vermote, E.F., Roger, J.-C., Skakun, S.V., Justice, C.O., 2018. The harmonized Landsat and Sentinel-2 surface reflectance data set. Remote Sens. Environ. 219, 145–161.

Cohen, W.B., Yang, Z., Healey, S.P., Kennedy, R.E., Gorelick, N., 2018. A LandTrendr multispectral ensemble for forest disturbance detection. Remote Sens. Environ. 205, 131–140.

DeVries, B., Decuyper, M., Verbesselt, J., Zeileis, A., Herold, M., Joseph, S., 2015. Tracking disturbance-regrowth dynamics in tropical forests using structural change detection and Landsat time series. Remote Sens. Environ. 169, 320–334.

Eerikäinen, K., Valkonen, S., Saksa, T., 2014. Ingrowth, survival and height growth of

small trees in uneven-aged Picea abies stands in southern Finland. For. Ecosyst. 1 (5). http://www.forestecosyst.com/1/1/5.
Ekö, P.-M., Johansson, U., Petersson, N., Bergqvist, J., Elfving, B., Frisk, J., 2008. Current growth differences of Norway spruce (Picea abies), Scots pine (Pinus sylvestris) and birch (Betula pendula and Betula pubescens) in different regions in Sweden. Scand. J. For. Res. 23 (4), 307–318.
FAO, 2012. FRA 2015: Terms and definitions. Forest Resource Assessment Working Paper 180. Food and Agriculture Organization of the United Nations, Rome, Italy Available online: (accessed July 18, 2018). http://www.fao.org/docrep/017/ap862e/ap862e00.pdf.
Fernandez-Delgado, M., Cernadas, E., Barro, S., Amorim, D., 2014. Do we need hundreds of classifiers to solve real world classification problems? Journal of Machine Learning Research 15, 3133–3181.
Finnish Forest Association, 2014. Forest Ownership. Available online: [accessed August 21, 2018.]. https://www.smy.fi/en/forest-fi/forest-facts/finnish-forests-owned-by-finns/.
Forest Stewardship Council Finland, 2010. FSC Standard for Finland. Available online:. https://fi.fsc.org/preview.fsc-standard-for-finland-v1-1-approved-210111.a-84.pdf.
Franklin, J.F., Spies, T.A., Van Pelt, R., Carey, A.B., Thornburgh, D.A., Berg, D.R., Lindenmayer, D.B., Harmon, M.E., Keeton, W.S., Shaw, D.C., Bible, K., Chen, J.Q., 2002. Disturbances and structural development of natural forest ecosystems with silvicultural implications, using Douglas-fir forests as an example. For. Ecol. Manage. 155, 399–423.
Frazier, R.J., Coops, N.C., Wulder, M.A., 2015. Boreal shield forest disturbance and recovery trends using Landsat time series. Remote Sens. Environ. 205, 32–45.
Frazier, R.J., Coops, N.C., Wulder, M.A., Hermosilla, T., White, J.C., 2018. Analyzing Spatial and Temporal Variability in Short-term Rates of Post-fire Vegetation Return From Landsat Time Series.
Frolking, S., Palace, M.W., Clark, D.B., Chambers, J.Q., Shugart, H.H., Hurtt, G.C., 2009. Forest disturbance and recovery: a general review in the context of spaceborne remote sensing of impacts on aboveground biomass and canopy structure. J. Geophys. Res. 114, 1–27.
Gatica-Saavedra, P., Echeverria, C., Nelson, C.R., 2017. Ecological indicators for assessing ecological success of forest restoration: a world review. Restor. Ecol. 25 (6), 850–857.
Griffiths, P., Kuemmerle, T., Baumann, M., Radeloff, V.C., Abrudan, I.V., Lieskovsky, J., Munteanu, C., Ostapowicz, K., Hostert, P., 2014. Forest disturbances, forest recovery, and changes in forest types across the Carpathian ecoregion from 1985 to 2010 based on Landsat image composites. Remote Sens. Environ. 151, 72–88.
Hansen, M.C., Potapov, P.V., Moore, R., Hancher, M., Turubanova, S.A., Tyukavina, A., Thau, D., Stehman, S.V., Goetz, S.J., Loveland, T.R., Kommareddy, A., Egorov, A., Chini, L., Justice, C.O., Townshend, J.R.G., 2013. High-resolution global maps of 21st-century forest cover change. Science 342, 850–853.
Hermosilla, T., Wulder, M.A., White, J.C., Coops, N.C., Hobart, G.W., 2015. An integrated Landsat time series protocol for change detection and generation of annual gap-free surface reflectance composites. Remote Sens. Environ. 158, 220–234.
Hermosilla, T., Wulder, M.A., White, J.C., Coops, N.C., Hobart, G.W., Campbell, L.B., 2016. Mass data processing of time series Landsat imagery: pixels to data products. Int. J. Digit. Earth 9 (11), 1035–1054.
Hermosilla, T., Wulder, M.A., White, J.C., Coops, N.C., Hobart, G.W., 2017. Updating Landsat time series of surface-reflectance composites and forest change products with new observations. Int. J. Appl. Earth Observ. 63, 104–111.
Holl, K.D., Aide, T.M., 2011. When and where to actively restore ecosystems? For. Ecol. Manage. 261 (10), 1558–1563.
Horler, D., Ahern, F., 1986. Forestry information content of Thematic Mapper data. Int. J. Remote Sens. 7, 405–428.
Ilvessalo, Y., Ilvessalo, M., 1975. Suomen metsätyypit metsiköiden luontaisen kehitys- ja puuntuottokyvyn valossa. Acta For. Fenn. 144, 1–101.
Johansson, K., Hajek, J., Sjölin, O., Normark, E., 2015. Early performance of *Pinus sylvestris* and *Picea abies* – a comparison between seedling size, species, and geographic location of the planting site. Scand. J. For. Res. 30 (5), 388–400.
Kankaanhuhta, V., 2014. Quality management of forest regeneration activities. Dissertation Forestales 174https://doi.org/10.14214/df.174. 93 p. Available at:.
Kankaanhuhta, V., Saksa, T., Smolander, H., 2009. Variation in the results of Norway spruce planting and Scots pine direct seeding in privately-owned forests in southern Finland. Silva Fenn. 43 (1), 51–70.
Kankaanhuhta, V., Saksa, T., Smolander, H., 2010. The effect of quality management on forest regeneration activities in privately-owned forests in southern Finland. Silva Fenn. 44 (2), 341–361.
Kennedy, R.E., Yang, Z., Cohen, W.B., Pfaff, E., Braaten, J., Nelson, P., 2012. Spatial and temporal patterns of forest disturbance and regrowth within the area of the Northwest Forest Plan. Remote Sens. Environ. 122, 117–133.
Korhonen, L., Pippuri, I., Packalén, P., Heikkinen, V., Maltamo, M., Heikkilä, J., 2013. Detection of the need for seedling stand tending using high-resolution remote sensing data. Silva Fenn. 47 (2), 1–20.
Kuhn, M., 2018. Caret: Classification and Regression Training, R Package Version 6.0-80. R Core Team, Vienna, Austria.
Kuhn, M., Johnson, K., 2013. Applied Predictive Modeling. Springer, New York, NJ, USA 2013.
Kuusinen, N., Stenberg, P., Tomppo, E., Bernier, P., Berninger, F., 2014. Variation in understory and canopy reflectance during stand development in Finnish coniferous forests. Can. J. For. Res. 45, 1077–1085.
Kuusinen, N., Stenberg, P., Korhonen, L., Rautiainen, M., Tomppo, E., 2016. Structural factors driving boreal forest albedo in Finland. Remote Sens. Environ. 175, 43–51.
Liaw, A., Wiener, M., 2002. Classification and regression by randomForest. R News 2, 18–22.
Liaw, A., Wiener, M., 2018. Randomforest, R Package Version 4.6-14. R Core Team, Vienna, Austria 2018.
Löfman, S., Kouki, J., 2001. Fifty years of landscape transformation in managed forests of Southern Finland. Scand. J. For. Res. 16 (1), 44–53.
Masek, J.G., Vermote, E.F., Saleous, N., Wolfe, R., Hall, F.G., Huemmrich, F., Gao, F., Kutler, J., Lim, T.K., 2006. A Landsat surface reflectance data set for North America, 1990–2000. IEEE Geosci. Remote. Sens. Lett. 3 (1), 68–72. https://doi.org/10.1109/LGRS.2005.857030.
Meli, P., Holl, K.D., Rey Benayas, J.M., Jones, H.P., Jones, P.C., Montoya, D., et al., 2017. A global review of past land use, climate, and active vs. passive restoration effects on forest recovery. PLoS One 12 (2), e0171368. https://doi.org/10.1371/journal.pone.0171368.
Miina, J., Saksa, T., 2013. Predicting establishment of tree seedlings in regeneration areas of Picea abies in Southern Finland. Balt. For. 19 (2), 187–200.
Miina, J., Turunen, J., Korhonen, K.T., Strandström, M., Ahola, A., 2018. Predicting the need for tending of conifer seedlings in southern Finland. Scand. J. For. Res. https://doi.org/10.1080/02827581.2018.1447681.
Miller, J.R., White, H.P., Chen, J.M., Peddle, D.R., McDermid, G., Fournier, R.A., Shepherd, P., Rubinstein, I., Freemantle, J., Soffer, R., LeDrew, E., 1997. Seasonal change in understory reflectance of boreal forests and influence on canopy vegetation indices. J. Geophys. Res. 102 (D24), 475–482.
Ministry of Agriculture and Forestry, 1996. Finland. Forest Act 1093/1996. Ministry of Agriculture and Forestry, Finland [accessed August 8, 2018]. https://www.finlex.fi/en/laki/kaannokset/1996/en19961093_20140567.pdf.
Ministry of Agriculture and Forestry, 2010. Forest Decree 1234/2010. [accessed August 8, 2018] In Finnish. https://www.finlex.fi/fi/laki/alkup/2010/20101234#Pidp446415648.
Mishra, N., Helder, D., Barsi, J., Markham, B., 2016. Continuous calibration improvement in solar reflective bands: Landsat 5 through Landsat 8. Remote Sens. Environ. 185, 7–15.
Natural Resources Institute Finland, 2017. Silvicultural and Forest Improvement Work. 2017. [cited August 15, 2018]. http://stat.luke.fi/en/silvicultural-and-forest-improvement-work.
Natural Resources Institute of Finland, 2015. The Multi-Source National Forest Inventory Raster Maps of 2013. Available at: [accessed June 1, 2017]. http://kartta.luke.fi/index-en.html.
Nilson, T., Peterson, U., 1994. Age dependence of forest reflectance: analysis of main driving factors. Remote Sens. Environ. 48, 319–331.
Nilsson, U., Luoranen, J., Kolström, T., Örlander, G., Puttonen, P., 2010. Reforestation with planting in northern Europe. Scand. J. For. Res. 25, 283–294.
Oliver, C.D., Larson, B.C., 1996. Forest Stand Dynamics (Updated Edition). John Wiley, New York.
Olsson, H., 2009. A method for using Landsat time series for monitoring young plantations in boreal forests. Int. J. Remote Sens. 30 (19), 5117–5131.
PEFC-Finland, 2014. Criteria for PEFC forest certification. PEFC FI 1002 (2014) Available online: https://www.pefc.org/images/stories/documents/NGB_Documentation/Finland/5_Criteria_for_Forest_Certification_PEFC_FI_1002_2014_eng_20141027.pdf.
Pflugmacher, D., Cohen, W.B., Kennedy, R.E., 2012. Using Landsat-derived disturbance history (1972-2010) to predict current forest structure. Remote Sensing of Environment 122, 146–165.
Pickell, P.D., Hermosilla, T., Frazier, R.J., Coops, N.C., Wulder, M.A., 2016. Forest recovery trends derived from Landsat time series for North American boreal forests. Int. J. Remote Sens. 37, 138–149.
Saarinen, N., White, J.C., Wulder, M.A., Kangas, A., Tuominen, S., Kankare, V., Holopainen, M., Hyyppä, J., Vastaranta, M., 2018. Landsat archive holdings for Finland: opportunities for forest monitoring. Silva Fenn. 52 (3), 9986.
Saksa, T., 2013. Regeneration after stump harvesting in southern Finland. For. Ecol. Manage. 290, 79–82.
Schmidt, G.L., Jenkerson, C.B., Masek, J., Vermote, E., Gao, F., 2013. Landsat Ecosystem Disturbance Adaptive Processing System (LEDAPS) Algorithm Description. U.S. Geological Survey Open-file Report 2013–1057. Available online:. pp. 17 p. http://pubs.usgs.gov/of/2013/1057/.
Schroeder, T.A., Cohen, W.B., Yang, Z., 2007. Patterns of forest regrowth following clearcutting in western Oregon as determined from Landsat time-series. For. Ecol. Manage. 243, 259–273.
Song, C., Schroeder, T.A., Cohen, W.B., 2007. Predicting temperate conifer forest successional stage distributions with multitemporal Landsat Thematic Mapper imagery. Remote Sens. Environ. 106, 228–237.
Spake, R., Ezard, T.H.G., Martin, P.A., Newton, A.C., Doncaster, C.P., 2015. A meta-analysis of functional group responses to forest recovery outside of the tropics. Conserv. Biol. 29 (6), 1695–1703.
Strobl, C., Boulesteix, A.L., Zeileis, A., Hothorn, T., 2007. Bias in random forest variable importance measures: illustrations, sources and a solution. BMC Bioinformatics 8 (25).
Strobl, C., Boulesteix, A.L., Kneib, T., Augustin, T., Zeileis, A., 2008. Conditional Variable Importance for Random Forests. BMC Bioinformatics (307), 9.
Strobl, C., Hothorn, T., Zeileis, A., 2009. Party on! A New Conditional Variable Importance Measure for Random Forests Available in the Party Package. Technical Report Number 050, Department of Statistics, University of Munich, pp. 4p.
Thompson, I.D., Guariguata, M.R., Okabe, K., Bahamondez, C., Nasi, R., Heymell, V., Sabogal, C., 2013. An operational framework for defining and monitoring forest degradation. Ecol. Soc. 18 (2), 20.
United Nations Environment Programme, 2019. Press Release: New UN Decade on Ecosystem Restoration Offers Unparalleled Opportunity for Job Creation, Food Security and Addressing Climate Change. Available online: (accessed April 9, 2019). https://www.unenvironment.org/news-and-stories/press-release/new-un-decade-ecosystem-restoration-offers-unparalleled-opportunity.

Urbano, A.R., Keeton, W.S., 2017. Carbon dynamics and structural development in recovering secondary forests of the northeastern U.S. For. Ecol. Manage. 392, 21–35.
Verdone, M., Seidl, A., 2017. Time, space, place, and the Bonn Challenge global forest restoration target. Restor. Ecol. 25 (6), 903–911.
White, J.C., Wulder, M.A., Hobart, G.W., Luther, J.E., Hermosilla, T., Griffiths, P., Coops, N.C., Hall, R.J., Hostert, P., Dyk, A., Guindon, L., 2014. Pixel-based image compositing for large-area dense time series applications and science. Can. J. Remote. Sens. 40 (3), 192–212.
White, J.C., Wulder, M.A., Hermosilla, T., Coops, N.C., Hobart, G., 2017. A nationwide annual characterization of 25 years of forest disturbance and recovery for Canada using Landsat time series. Remote Sens. Environ. 194, 303–321.
White, J.C., Saarinen, N., Kankare, V., Wulder, M.A., Hermosilla, T., Coops, N.C., Pickell, P.D., Holopainen, M., Hyyppä, J., Vastaranta, M., 2018. Confirmation of post-harvest spectral recovery from Landsat time series using measures of forest cover and height derived from airborne laser scanning data. Remote Sens. Environ. 216, 262–275.
Woodcock, C.E., Allen, R., Anderson, M., Belward, A., Bindschadler, R., Cohen, W., Gao, F., Goward, S.N., Helder, D., Helmer, E., Nemani, R., Oreopoulos, L., Schott, J., Thenkabail, P.S., Vermote, E.F., Vogelmann, J., Wulder, M.A., Wynne, R., 2008. Free access to Landsat imagery. Science 320 (5874), 1011.
Wulder, M.A., Hilker, T., White, J.C., Coops, N.C., Masek, J.G., Pflugmacher, D., Crevier, Y., 2015. Virtual constellations for global terrestrial monitoring. Remote Sens. Environ. 170, 62–76.
Wulder, M.A., Loveland, T.R., Roy, D.P., Crawford, C.J., Zhu, Z., 2019. Current status of Landsat program, science, and applications. Remote Sens. Environ. 225, 127–147.
Zhu, Z., Woodcock, C.E., 2012. Object-based cloud and cloud shadow detection in Landsat imagery. Remote Sens. Environ. 118, 83–94. https://doi.org/10.1016/j.rse.2011.10.028.